Talanta 85 (2011) 76–81

Contents lists available at ScienceDirect

Talanta

journal homepage: www.elsevier.com/locate/talanta

Functionalization of graphene with electrodeposited Prussian blue towards amperometric sensing application

Yuanyuan Jiang[a], Xindong Zhang[a], Changsheng Shan[a], Shucheng Hua[b,*], Qixian Zhang[a], Xiaoxue Bai[b], Li Dan[b], Li Niu[a,b,**]

[a] Engineering Laboratory for Modern Analytical Techniques, c/o State Key Laboratory of Electroanalytical Chemistry, Changchun Institute of Applied Chemistry, Graduate University of the Chinese Academy of Sciences, Chinese Academy of Sciences, Changchun 130022, PR China
[b] College of Chemistry and Norman Bethune College of Medicine, Jilin University, Changchun 130021, PR China

ARTICLE INFO

Article history:
Received 20 December 2010
Received in revised form 5 March 2011
Accepted 12 March 2011
Available online 23 March 2011

Keywords:
Graphene
Functionalization
Prussian blue
Amperometric sensing

ABSTRACT

Prussian blue (PB) was grown compactly on graphene matrix by electrochemical deposition. The as-prepared PB-graphene modified glassy carbon electrode (PB-graphene/GCE) showed excellent electrocatalytic activity towards both the reduction of hydrogen peroxide and the oxidation of hydrazine, which could be attributed to the remarkable synergistic effect of graphene and PB. The PB-graphene/GCE showed sensitive response to H_2O_2 with a wide linear range of 10–1440 μM at 0.0 V, and to hydrazine with a wide linear range of 10–3000 μM at 0.35 V. The detection limit was 3 μM and 7 μM, respectively, and both of them had rapid response within 5 s to reach 95% steady state response. The wide linear range, good selectivity and long-time stability of the PB-graphene/GCE make it possible for the practical amperometric detection of hydrogen peroxide and hydrazine.

1. Introduction

Graphene is the name given to a two-dimensional sheet of sp^2-hybridized carbon. Since Geim and Novoselov at Manchester University first exfoliated single-layer graphene from graphite [1], explosion of interest has occurred to both the theoretical and experimental scientists. Owing to its unique electrical, mechanical, and thermal properties, graphene has found many application areas, such as energy-storage materials [2], free-standing paper-like materials [3], polymer composites [4], liquid crystal devices [5], mechanical resonators [6], and electrochemical sensors [7,8]. Many approaches have been developed for preparing graphene, such as scotch tape (peel off) method [9], epitaxial growth [10], chemical vapor deposition (CVD) [11], solvent thermal reaction [12], graphite intercalation compounds (GIC) [13] and the chemical reduction of graphene oxide (GO) [14,15]. Based on its feasibility of mass production, the oxidation and reduction of graphite is one of the most effective methods to prepare graphene sheets. Most of graphene sheets used in electrochemistry are produced with this method. Graphene obtained from GO reduction, which is also called chemically reduced GO, usually has plentiful structural defects [16] and functional groups [14]. These features are advantageous for its electrochemical applications [17]. Carbon might be the most widely used material in electroanalysis and electrocatalysis. For example, carbon nanotubes (CNTs) have shown excellent performance in electrochemical sensors [18,19]. It is believed that graphene-based electrodes may have superior performance in terms of electrocatalytic activity [20] and macroscopic scale conductivity [21] than CNTs-based ones. These indicate that the opportunities in electrochemistry dealing with CNTs might be available for graphene.

Prussian blue (PB), $Fe_4[Fe(CN)_6]_3$, has perfect catalytic activity towards some low molecular weight molecules (such as O_2, H_2O_2, hydrazine) due to its unique zeolite structure. Since Itaya, et al. demonstrated that the reduced form of PB (Prussian white, PW) showed catalytic activity for the reduction of oxygen and hydrogen peroxide in 1984 [22], PB-based electrochemical sensors have been widely investigated, especially in the catalysis for H_2O_2 reduction. It was reported that for the optimized conditions, the calculated bimolecular rate constant for the reduction of H_2O_2 was $3 \times 10^3\ M^{-1}\ s^{-1}$ [23–25], which was very similar to that measured for the peroxidase enzyme ($2 \times 10^4\ M^{-1}\ s^{-1}$) [26]. Electrochemical properties such as formal potential, sensitivity, stability and electron transfer rate constants of the PB and its corresponding redox state depend on deposition method, pH, molecular structure and concentration of the supporting electrolyte, etc. [27,28].

* Corresponding author. Fax: +86 431 8526 2800.
** Corresponding author at: Engineering Laboratory for Modern Analytical Techniques, c/o State Key Laboratory of Electroanalytical Chemistry, Changchun Institute of Applied Chemistry, Graduate University of the Chinese Academy of Sciences, Chinese Academy of Sciences, Renmin St. 5625, Changchun 130022, PR China. Fax: +86 431 8526 2800.
E-mail addresses: huashucheng@jlu.edu.cn (S. Hua), lniu@ciac.jl.cn (L. Niu).

0039-9140/$ – see front matter © 2011 Elsevier B.V. All rights reserved.
doi:10.1016/j.talanta.2011.03.028

The principal handicap in application of PB is its high solubility at neutral and basic pH, although it shows good sensitivity and stability in acid conditions. One approach to improving this situation is by changing the deposition procedure, thus slightly modifying the three-dimensional structure of PB and avoiding OH^- diffusion across the crystal. However, a more practical approach might be the use of protective polymer films coated over PB to enhance both its stability and selectivity against other electroactive interfering substances. Several polymers have been widely used, such as Nafion, polypyrrole, polyaniline [29,30].

To realize its application, high quality supporters are usually required for the immobilization of PB. Many efforts have been devoted to preparing new supporting materials. Among these materials, CNTs have been most widely studied because of their particular nanostructure, outstanding electron-transfer capacity, and good stability [31,32]. However, preparation, purification and functionalization of CNTs are really harsh processes, which limit their further application. Considering the remarkable properties of graphene and its relatively easy preparation approach, undoubtedly, combining PB with graphene sheets should be a powerful method for immobilizing PB.

In this work, we prepared graphene sheets by mild chemical reduction of GO, and PB was electrodeposited onto the graphene matrix by cyclic voltammetry scanning. To the best of our knowledge, it is the first time to electrodeposit PB on graphene matrix, and apply the resulting composite as electrochemical sensor. This modified electrode had excellent electrocatalytic activity towards both the reduction of H_2O_2 and the oxidation of hydrazine. And the PB-graphene/GCE had long-term stability without the use of protective polymer films.

2. Experimental

2.1. Reagents

Graphite powders (320 mesh) were of spectroscopic purity and were purchased from Shanghai Chemicals, China. Hydrazine solution (50 wt%) and ammonia solution (28 wt%) were obtained from Sinopharm Chemical Reagent Co., Ltd. Hydrogen peroxide (30 wt%) and other regents were purchased from Beijing Chemical Regent Plant (Beijing, China). Unless otherwise stated, the regents used in the experiment were of analytical grade and used as received without further purification. Diluted H_2O_2 and hydrazine solution were freshly prepared before use. Phosphate buffer solution (PBS, 0.05 M, pH 6.0) used as supporting electrolyte was prepared from KH_2PO_4 and K_2HPO_4. Aqueous solutions were prepared with double-distilled water from a Millipore system (>18 MΩ cm).

2.2. Instruments

The morphology of the modified electrode was analyzed with a field emission scanning electron microscope (FE-SEM, XL30ESEM-FEG) at a accelerate voltage of 20.0 kV. X-ray photoelectron spectroscopy (XPS) analysis was carried out on an ESCALAB MK II X-ray photoelectron spectrometer. UV–vis spectra were recorded on a Cary 500 UV–vis spectrometer (Varian) on indium tin oxide (ITO) slide in the range of 400–800 nm. Cyclic voltammetric (CV) measurements were performed with a DC-EC Electrochemical Workstation (DyneChem, China) in a conventional three-electrode system with bare or modified GCE (d = 3 mm) as working electrode, a platinum wire as the counter electrode and an Ag|AgCl (saturated KCl) as reference. Before use, GCE was carefully polished to a mirror finish with 1.0, 0.3, and 0.05 μm alumina slurries successively, and rinsed with deionized water, followed by sonication in acetone and deionized water in succession, and finally dried in N_2.

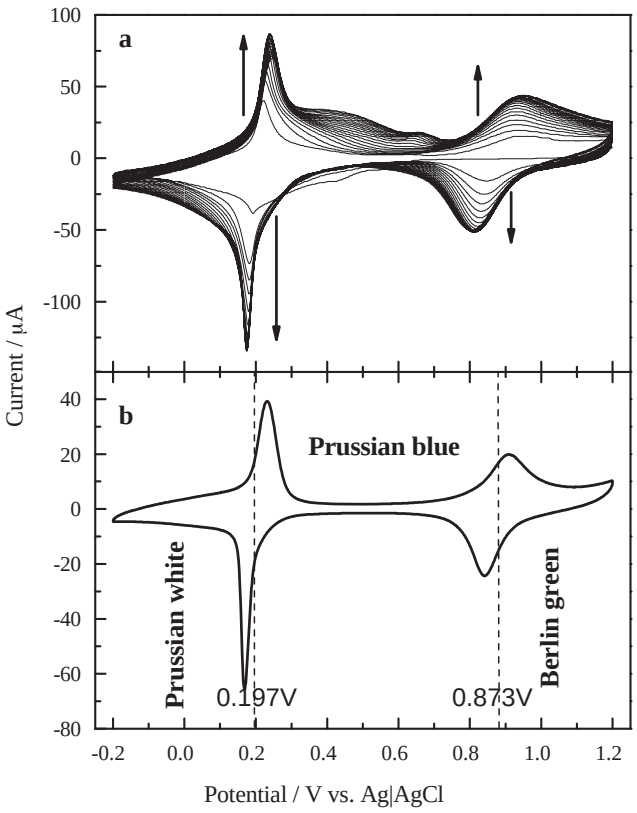

Fig. 1. (a) Growth process of PB film on the graphene coated GCE in a solution composed of 2 mM $FeCl_3$, 2 mM $K_3[Fe(CN)_6]$, 0.1 M KCl and 0.01 M HCl. Scan rate: 50 mV s^{-1}. (b) Cyclic voltammogram of PB-graphene/GCE in PBS (0.05 M, pH 6.0) containing 0.1 M KCl at 50 mV s^{-1}.

2.3. Preparation of the PB-graphene modified electrode

2.3.1. Preparation of water soluble graphene sheets

GO was prepared according to a modified Hummers and Offeman method [33,34]. Then in a typical procedure for chemical conversion of GO to graphene, 5 mL of 0.5 mg/mL GO was mixed with 5 mL water and 3.5 μL hydrazine solution (50 wt% in water). Ammonia solution (28 wt% in water) was dropped into the mixed solution to adjust the pH to 10.0. After being vigorously shaken or stirred for a few minutes, the mixture was refluxed for an hour under a oil bath (95 °C). The resulting homogeneous solution was purified by dialysis for 3 days. The weight ratio of hydrazine to GO was 7:10, and the reaction time is 1 h in the experiment. This condition appears to be an optimal situation for producing stable dispersion of highly conductive graphene sheets, according to a previous report [15].

2.3.2. Electrodeposition of PB on graphene modified glassy carbon electrode

The cleaned GCE was coated with a suspension (5 μL) of the as-prepared graphene, and allowed to be dried under an infrared lamp. PB-graphene/GCE was prepared by means of electrodeposition and subsequent activation. The PB particles were electrodeposited using cyclic voltammetry scanning by applying 20 cyclic scans within the limits of −0.20 to 1.20 V (vs. Ag|AgCl) at a scan rate of 50 mV s^{-1} in a freshly deaerated solution containing 2 mM $FeCl_3$, 2 mM $K_3[Fe(CN)_6]$, 0.1 M KCl and 0.01 M HCl. Afterward, the modified electrode was thoroughly rinsed with deionized water to remove unwanted ions by weak physical absorption. Then the PB-graphene modified electrode was activated by applying another 10 CV cycles in deaerated electrolyte solution (0.1 M KCl and 0.01 M

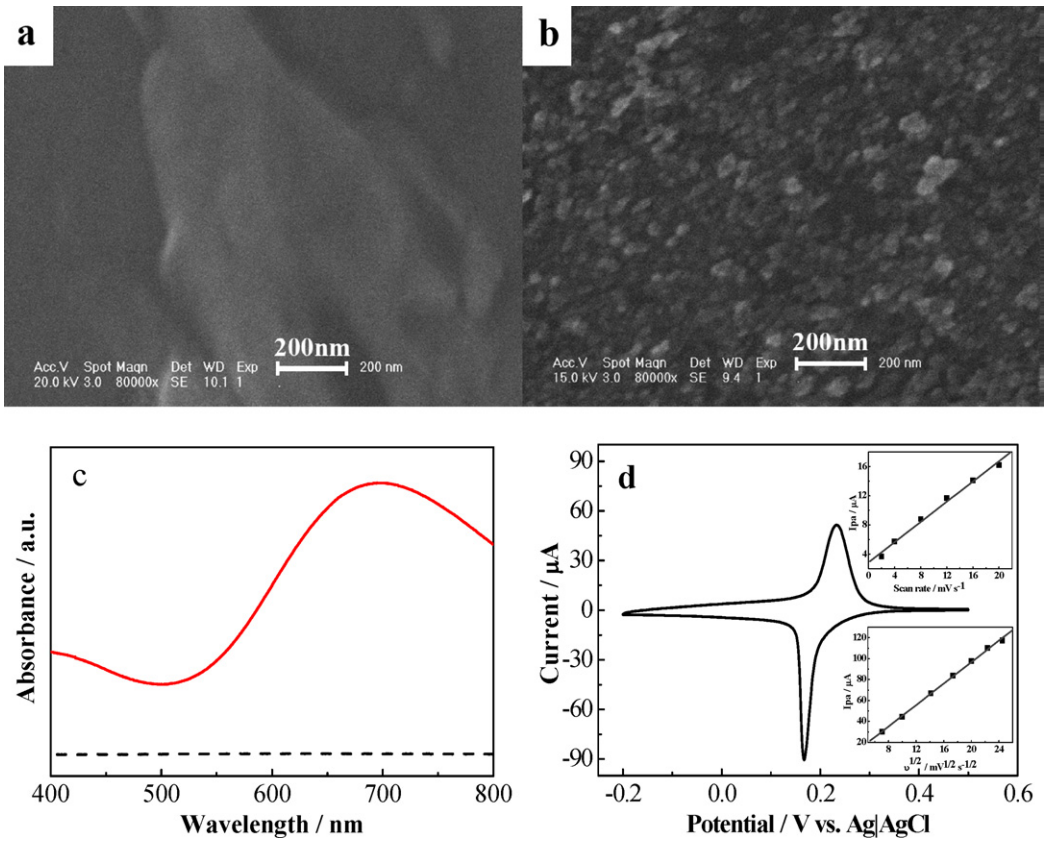

Fig. 2. SEM images of graphene/GCE (a) and PB-graphene/GCE (b); (c) absorbance spectra of PB-graphene and (solid) and graphene (dashed); (d) the first cyclic voltammogram peaks of PB-graphene/GCE at 50 mV s^{-1}. Inset, upper-right: plot of the peak current at ca. 0.17 V versus the scan rate in the range 2–20 mV s^{-1}. Inset, lower-right: plot of the peak current at ca. 0.17 V versus the square root of the scan rate in the range 50–600 mV s^{-1}. Supporting electrolyte is PBS (0.05 M, pH 6.0) containing 0.1 M KCl.

HCl) from −0.2 to 0.5 V. Finally, the PB film was tempered at 100 °C for 1 h to stabilize the formed PB layer [30].

3. Results and discussion

3.1. Characterization of PB-graphene modified electrode

The graphene oxide and graphene were characterized by XPS (Fig. S1). The C1s XPS spectrum of graphene showed similar elements and functional groups with graphene oxide, however, a greatly decreased amount of C in epoxy groups was observed clearly after reduction. In addition, there was an additional component at 285.8 eV, corresponding to the carbon in C–N bonds. Fig. 1a shows the growth process of the PB film. Two pairs of redox waves appeared at formal potential ($E^{\circ\prime}$) of 0.208 V and 0.875 V, respectively. All redox peaks gradually grew and the peak potentials remained relatively constant with the increasing of the scan cycle. These phenomena demonstrated that the PB film had formed on the graphene/GCE substrate successfully. After activation and stabilization, the PB-graphene/GCE was examined in the blank PBS electrolyte (0.05 M, pH 6.0) containing 0.1 M KCl, and the resulting CV curve is shown in Fig. 1b. Two pairs of typical redox waves showing the oxidation of PB to Berlin green (BG) as well as the reduction of PB to Prussian white (PW) were observed for the PB-graphene/GCE, indicating the effective presence of PB on the modified electrode. The formal potentials ($E^{\circ\prime}$) calculated by averaging the cathodic and anodic peak potential was found to be 0.197 V for the redox conversion between PB and PW, and 0.873 V for the redox conversion between PB and BG. The peak-to-peak separation (ΔE_p) was 66 mV in both situations, indicating a clear mono-electronic and quasi-reversible behavior. The results were in good accordance with the previous reports [35,36]. The conversion processes of the two redox pairs were shown as follows:

$$(PB)\,Fe(III)_4[Fe(II)(CN)_6]_3 + 4e^- + 4K^+ \rightarrow (PW)\,K_4Fe(II)_4[Fe(II)(CN)_6]_3 \quad (1)$$

$$(PB)\,Fe(III)_4[Fe(II)(CN)_6]_3 + 3Cl^- \rightarrow (BG)\,Fe(III)_4[Fe(III)(CN)_6]_3Cl_3 + 3e^- \quad (2)$$

SEM was used to characterize the morphologies of the graphene/GCE, and PB-graphene/GCE. As shown in Fig. 2a, planar graphene sheets were well distributed on the GCE surface. The graphene sheets with high specific surface area and crumpled structure were beneficial for the further immobilization of PB and the performance of the modified electrode. Fig. 2b demonstrated that the PB nanoparticles were electrochemically deposited on the surface of graphene modified electrode with the diameter about 30–50 nm. Some larger particles could also been seen on the graphene surface, which seemed to be the accumulation of the PB nanoparticles. The SEM images indicated that the electrochemical deposition of PB on graphene surface was applicable. Absorbance spectrum (Fig. 2c) of the as-deposited PB film showed the characteristic broad absorption peak centered at 672 nm due to charge transfer between Fe^{3+} and Fe^{2+} ions, as reported by other authors [37,38].

The influence of the scan rates on the reduction peak current at ca. 0.17 V was investigated. Fig. 2d showed the CV of the PB-graphene/GCE in N_2-saturated PBS (0.05 M, pH 6.0) containing 0.1 M KCl at a scan rate of 50 mV s^{-1}, and the influence of scan rates on cathodic peak current. As expected, a linear relationship of the cathodic peak current of PB as a function of the scan rates between 2 and 20 mV s^{-1} was observed (Fig. 2d, inset, upper-right), indicating that the observed electrochemical reactions were a surface-confined process. At higher scan rates up to 600 mV s^{-1}, the peak current was proportional to the square root of the scan rate, as shown in Fig. 2d (inset, lower-right). This indicated that

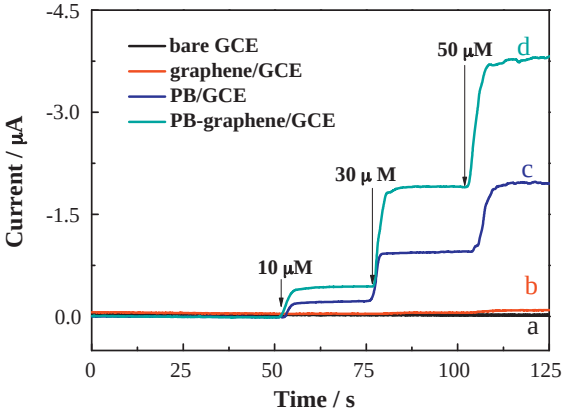

Fig. 3. Amperometric response recorded at bare GCE (a), graphene/GCE (b), PB/GCE (c) and PB-graphene/GCE (d) with the addition of 10, 30, 50 μM H_2O_2 to stirring N_2-saturated PBS. *Condition*: in 0.05 M PBS (pH 6.0) containing 0.1 M KCl at 0.0 V.

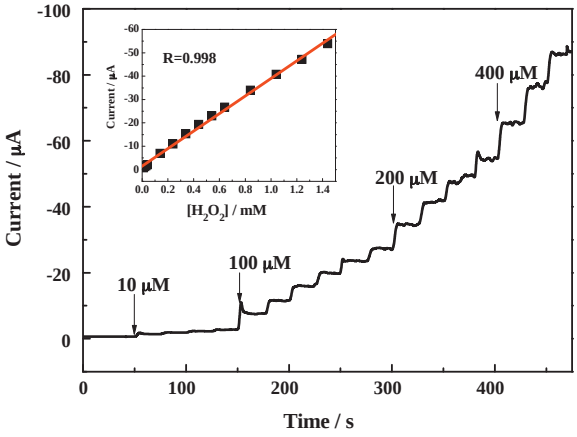

Fig. 4. Amperometric response of PB-graphene/GCE with successive injection of H_2O_2. *Inset*: calibration curve of H_2O_2 concentration on the modified electrode. *Condition*: the same as in Fig. 3.

the reaction kinetics changed from a surface-confined process to a diffusion-limited process. These results are in good agreement with those previously reported literatures [39,40].

3.2. PB-graphene/GCE for H_2O_2 electrochemical detection

The PB-graphene/GCE showed high electrocatalytic activity towards the reduction of H_2O_2 in optimized conditions. PBS (prepared from KH_2PO_4 and K_2HPO_4) containing 0.1 M KCl was used as electrolyte because only cations with small hydrated radii, such as K^+, NH_4^+, Rb^+ and Cs^+, could support this electrochemical activity by diffusing across the PB structure. The pH value of the supporting electrolyte was selected at pH 6.0, because the current response is distinct, and PB is not soluble at this pH, while at higher pH, the as-prepared PB film can be dissolved partially (not shown in the paper). The CV curves of the PB-graphene/GCE in N_2-saturated PBS with and without the addition of H_2O_2 are shown in Fig. S2. Taking sensitive response, operational stability and effective avoiding interference into account, 0.0 V was selected as the applied potential for H_2O_2 electrochemical detection.

In the control experiment (Fig. 3), the responses to H_2O_2 on a bare GCE (curve *a*), graphene/GCE (curve *b*) and PB/GCE (curve *c*) were compared to that on PB-graphene/GCE (curve *d*). The bare GCE showed hardly catalytic effect towards H_2O_2 reduction and graphene/GCE yielded detectable but very small current response. The presence of the current at the PB/GCE was due to the mediated redox process of PB nanoparticles. When PB was electrodeposited on the graphene matrix, a two-fold current response could be observed clearly due to the synergistic effect of PB and graphene.

Fig. 4 shows a typical steady state response of the PB-graphene/GCE on successive addition of H_2O_2 at 0.0 V in stirring PBS. Upon addition of the H_2O_2 solution, a rapid increase in the cathodic current occurred as the reduction of the hydrogen peroxide. The current response of the modified electrode reached 95% of the steady-state current within 5 s. The current response increased linearly with the H_2O_2 concentration. The inset of Fig. 4 showed the calibration curve of H_2O_2 at the modified electrode. The PB-graphene/GCE had a linear response to H_2O_2 in the range of 10–1440 μM with a correlation coefficient of 0.998. The sensitivity of the modified electrode was 0.53 $\mu A\,\mu M^{-1}\,cm^{-2}$ H_2O_2 with a detection limit 3 μM at the signal-to-noise ratio of 3.

3.3. PB-graphene/GCE for hydrazine electrochemical detection

Hydrazine (N_2H_4) and its derivatives have received a growing amount of attention due to their wide application in many fields, such as industrial, agriculture, pharmacological, military and aerospace area [41]. However, hydrazine is toxic and has been recognized as carcinogenic and hepatotoxic substance, which causes liver and kidney damages [42]. Therefore fast and accurate detection of hydrazine is of great importance. Due to its high sensitivity, good selectivity, portable, economical and simple operating procedure, electrochemical technique is a competitive alternative for the determination of hydrazine. Unfortunately, the direct oxidation of hydrazine at bare electrode is not suited for analytical application due to slow electrode kinetics and high overpotential [43].

Here, the PB-graphene/GCE can reduce the overpotential of hydrazine oxidation evidently with the onset potential at 0.05 V and peak potential at 0.22 V. 0.35 V was selected as the operating potential in the potentiostatic experiment, as the electrocatalytic effect was more obvious at this potential (shown in Fig. S3). From the control experiment (Fig. 5), it could be observed that the graphene/GCE (a) and PB/GCE (b) both had electrocatalytic effect on the similar scale towards the oxidation of hydrazine, while the bare GCE (a) could hardly catalyze the oxidation process. When PB nanoparticles were electrodeposited onto the graphene surface, the current response increased evidently because of the synergistic effect of graphene and PB.

The amperometric response of the PB-graphene/GCE at a potential of 0.35 V is shown in Fig. 6. The catalytic current increased fleetly with the addition of hydrazine solution. About 5 s were needed to

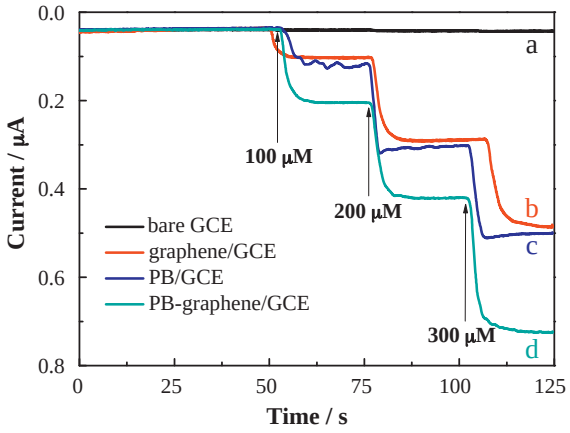

Fig. 5. Amperometric response recorded at bare GCE (a), graphene/GCE (b), PB/GCE (c) and PB-graphene/GCE (d) with the addition of 100, 200, 300 μM hydrazine to stirring N_2-saturated PBS (0.05 M, pH 6.0, containing 0.1 M KCl) at 0.35 V.

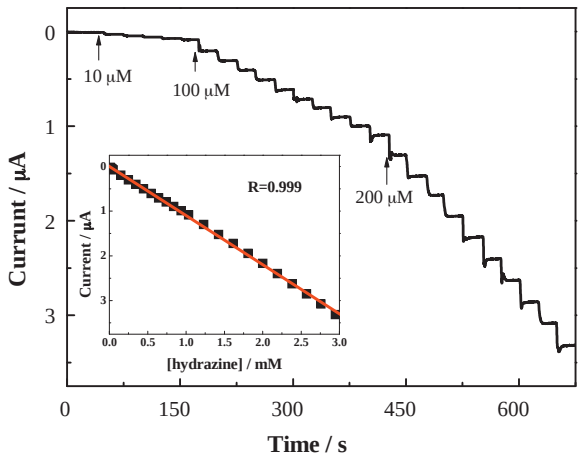

Fig. 6. Amperometric response of PB-graphene/GCE with successive injection of hydrazine into a stirring N_2-saturated PBS at 0.35 V. *Inset*: calibration curve of hydrazine concentration on the modified electrode. *Conditions*: the same as in Fig. 5.

reach 95% of the steady-state current. The electrochemical response to hydrazine showed a wide linear range of 10–3000 μM (R = 0.999) and a detection limit of 7 μM.

3.4. Stability and reproducibility of the PB-graphene/GCE

The reproducibility and stability of the modified electrode were investigated. The relative standard deviation (RSD) of the current response was 3.8% for 8 successive determinations to 1 mM H_2O_2, and 3.5% to 1 mM hydrazine. After stored in dry and airtight environment for a week, the current response maintained 90% towards the reduction of H_2O_2 and 93% towards the hydrazine oxidation. It can be interpreted that the graphene sheets have planar structure with high specific surface and crumpled segments, which are well-suited for electrodepositing compact nanostructured PB, and maintain its forceful immobilization. The unique structure of graphene matrix and the optimization of the experimental conditions, make the as-prepared PB-graphene/GCE a potential electrochemical sensor for both H_2O_2 reduction and hydrazine oxidation detections with satisfying stability and reproducibility.

3.5. Interference study and determination of hydrazine in real samples

A problem which should not be neglected in the determination of hydrazine is the potential interference caused by coexisted ions in environmental system and electroactive species containing nitrogen, such as nitrate, nitrite and ammonium, which may accompany with hydrazine in some industrial processes [44,45]. To evaluate the selectivity of the proposed sensor, the effect of the presence of 100-fold of common ions (Cl^-, $C_2O_4^{2-}$, SO_4^{2-}, NO_3^-, NO_2^-, PO_4^{3-} Ca^{2+}, Na^+, NH_4^+, Mg^{2+}, K^+, Cu^{2+},) which may coexist with hydrazine in real samples on the current intensity of the proposed sensor towards 100 μM hydrazine was investigated. As shown in Fig. S4, no obvious interference was observed from the mentioned species with a 5% error criterion.

The proposed sensor was applied for determination of hydrazine in spiked tap water and mineral water under optimized conditions. Table 1 shows the results obtained for three parallel measurements. The results indicated that the proposed method could be used for hydrazine determination in real samples.

Table 1
Determination of hydrazine in different water samples using proposed sensor.

Sample	Hydrazine added (μM)	Hydrazine found (μM) [a]	Recovery (%)
Tap water	50	51.75	103.5
	100	106.0	106.0
	150	154.0	102.7
Mineral water	50	49.70	99.40
	100	103.2	103.2
	150	155.5	103.7

[a] Average of three determinations.

4. Conclusions

Prussian blue nanoparticles were deposited successfully onto graphene modified GCE by electrochemical method. The PB-graphene/GCE had admirable electrocatalytical performance towards both the reduction of H_2O_2 and the oxidation of hydrazine. Both of the situations can be attributed to the unique zeolite structure of PB which allowed molecules (H_2O_2 and hydrazine) with low molecular weight and scale to penetrate into the crystal and achieve well electrocatalysis. Besides, the incorporation of PB onto a graphene modified electrode resulted in a distinct increase of the response current compared to PB modified electrode. It was confirmed that the increased amperometric response was due to the synergistic effect of graphene and PB. The fast response and wide linear range of the graphene-PB/GCE in both situations make it possible to use the PB-graphene/GCE as hydrogen peroxide sensor and hydrazine sensor. Such graphene-PB modified electrode can be further constructed as chemosensors and/or biosensors, and the in-depth investigation is under the way.

Acknowledgements

The authors are most grateful to the NSFC, China (nos. 20673109, 20827004), the Department of Science and Technology of Jilin Province (no. 20080518) and Chinese Academy of Science (KGCX2-YW-231, and YZ200906, YZ2010018) for their financial support.

Appendix A. Supplementary data

Supplementary data associated with this article can be found, in the online version, at doi:10.1016/j.talanta.2011.03.028.

References

[1] A.K. Geim, K.S. Novoselov, Nat. Mater. 6 (2007) 183.
[2] M.D. Stoller, S.J. Park, Y.W. Zhu, J.H. An, R.S. Ruoff, Nano Lett. 8 (2008) 3498.
[3] D.A. Dikin, S. Stankovich, E.J. Zimney, R.D. Piner, G.H.B. Dommett, G. Evmenenko, S.T. Nguyen, R.S. Ruoff, Nature 448 (2007) 457.
[4] S. Stankovich, D.A. Dikin, G.H.B. Dommett, K.M. Kohlhaas, E.J. Zimney, E.A. Stach, R.D. Piner, S.T. Nguyen, R.S. Ruoff, Nature 442 (2006) 282.
[5] P. Blake, P.D. Brimicombe, R.R. Nair, T.J. Booth, D. Jiang, F. Schedin, L.A. Ponomarenko, S.V. Morozov, H.F. Gleeson, E.W. Hill, A.K. Geim, K.S. Novoselov, Nano Lett. 8 (2008) 1704.
[6] D. Garcia-Sanchez, A.M. van der Zande, A.S. Paulo, B. Lassagne, P.L. McEuen, A. Bachtold, Nano Lett. 8 (2008) 1399.
[7] X.H. Kang, J. Wang, H. Wu, I.A. Aksay, J. Liu, Y.H. Lin, Biosens. Bioelectron. 25 (2009) 901.
[8] C.S. Shan, H.F. Yang, J.F. Song, D.X. Han, A. Ivaska, L. Niu, Anal. Chem. 81 (2009) 2378.
[9] K.S. Novoselov, A.K. Geim, S.V. Morozov, D. Jiang, Y. Zhang, S.V. Dubonos, I.V. Grigorieva, A.A. Firsov, Science 306 (2004) 666.
[10] C. Berger, Z.M. Song, X.B. Li, X.S. Wu, N. Brown, C. Naud, D. Mayou, T.B. Li, J. Hass, A.N. Marchenkov, E.H. Conrad, P.N. First, W.A. de Heer, Science 312 (2006) 1191.
[11] J.J. Wang, M.Y. Zhu, R.A. Outlaw, X. Zhao, D.M. Manos, B.C. Holloway, Carbon 42 (2004) 2867.
[12] C. Nethravathi, M. Rajamathi, Carbon 46 (2008) 1994.
[13] Z.P. Zhu, D.S. Su, G. Weinberg, R. Schlogl, Nano Lett. 4 (2004) 2255.
[14] S. Stankovich, D.A. Dikin, R.D. Piner, K.A. Kohlhaas, A. Kleinhammes, Y. Jia, Y. Wu, S.T. Nguyen, R.S. Ruoff, Carbon 45 (2007) 1558.

[15] D. Li, M.B. Muller, S. Gilje, R.B. Kaner, G.G. Wallace, Nat. Nanotechnol. 3 (2008) 101.
[16] S. Park, R.S. Ruoff, Nat. Nanotechnol. 4 (2009) 217.
[17] R.L. McCreery, Chem. Rev. 108 (2008) 2646.
[18] J. Wang, Electroanalysis 17 (2005) 7.
[19] Y.H. Lin, F. Lu, Y. Tu, Z.F. Ren, Nano Lett. 4 (2004) 191.
[20] Y. Wang, Y.M. Li, L.H. Tang, J. Lu, J.H. Li, Electrochem. Commun. 11 (2009) 889.
[21] S. Alwarappan, A. Erdem, C. Liu, C.Z. Li, J. Phys. Chem. C 113 (2009) 8853.
[22] K. Itaya, N. Shoji, I. Uchida, J. Am. Chem. Soc. 106 (1984) 3423.
[23] A.A. Karyakin, E.E. Karyakina, L. Gorton, Anal. Chem. 72 (2000) 1720.
[24] A.A. Karyakin, E.E. Karyakina, L. Gorton, Talanta 43 (1996) 1597.
[25] A.A. Karyakin, E.E. Karyakina, Sens. Actuators B 57 (1999) 268.
[26] B.B. Hasinoff, H.B. Dunford, Biochemistry 9 (1970) 4930.
[27] J. Kawiak, T. Jedral, Z. Galus, J. Electroanal. Chem. 145 (1983) 163.
[28] L. Li, Q.L. Sheng, J.B. Zheng, H.F. Zhang, Bioelectrochemistry 74 (2008) 170.
[29] Q.J. Chi, S.J. Dong, Anal. Chim. Acta 310 (1995) 429.
[30] F. Ricci, G. Palleschi, Biosens. Bioelectron. 21 (2005) 389.
[31] L. Wang, S.J. Guo, X.O. Hu, S.J. Dong, Colloids Surf. A 317 (2008) 394.
[32] D. Du, M.H. Wang, Y.H. Qin, Y.H. Lin, J. Mater. Chem. 20 (2010) 1532.
[33] W.S. Hummers, R.E. Offeman, J. Am. Chem. Soc. 80 (1958) 1339.
[34] N.I. Kovtyukhova, P.J. Ollivier, B.R. Martin, T.E. Mallouk, S.A. Chizhik, E.V. Buzaneva, A.D. Gorchinskiy, Chem. Mater. 11 (1999) 771.
[35] K. Itaya, T. Ataka, S. Toshima, J. Am. Chem. Soc. 104 (1982) 4767.
[36] A.A. Karyakin, Electroanalysis 13 (2001) 813.
[37] Y.L. Hu, J.H. Yuan, W. Chen, K. Wang, X.H. Xia, Electrochem. Commun. 7 (2005) 1252.
[38] P. Salazar, M. Martin, R. Roche, R.D. O'Neill, J.L. Gonzalez-Mora, Electrochim. Acta 55 (2010) 6476.
[39] N.F. Zakharchuk, B. Meyer, H. Hennig, F. Scholz, A. Jaworksi, Z. Stojek, J. Electroanal. Chem. 398 (1995) 23.
[40] J. Li, J.D. Qiu, J.J. Xu, H.Y. Chen, X.H. Xia, Adv. Funct. Mater. 17 (2007) 1574.
[41] A. Umar, M.M. Rahman, Y.B. Hahn, Talanta 77 (2009) 1376.
[42] C. Wang, L. Zhang, Z.H. Guo, J.G. Xu, H.Y. Wang, K.F. Zhai, X. Zhuo, Microchim. Acta 169 (2010) 1.
[43] G.F. Wang, A.X. Gu, W. Wang, Y. Wei, J.J. Wu, G.Z. Wang, X.J. Zhang, B. Fang, Electrochem. Commun. 11 (2009) 631.
[44] H.J. Yang, B.P. Lu, L.P. Guo, B. Qi, J. Electroanal. Chem. 650 (2011) 171.
[45] B. Haghighi, H. Hamidi, S. Bozorgzadeh, Anal. Bioanal. Chem. 398 (2010) 1411.